Centromere-localized breaks indicate the generation of DNA damage by the mitotic spindle

Astrid Alonso Guerrero[a], Mercedes Cano Gamero[a], Varvara Trachana[a,1], Agnes Fütterer[a], Cristina Pacios-Bras[a], Nuria Panadero Díaz-Concha[a], Juan Cruz Cigudosa[b], Carlos Martínez-A.[a], and Karel H.M. van Wely[a,2]

[a]Department of Immunology and Oncology, Centro Nacional de Biotecnología/Consejo Superior de Investigaciones Científicas, Universidad Autónoma de Madrid, Cantoblanco Campus, 28049 Madrid, Spain; and [b]Molecular Cytogenetics Group, Human Cancer Genetics Program, Spanish National Cancer Center, 28029 Madrid, Spain

Communicated by A. Garcia-Bellido, Universidad Autónoma de Madrid, Madrid, Spain, October 30, 2009 (received for review June 1, 2009)

Most carcinomas present some form of chromosome instability in combination with spindle defects. Numerical instability is likely caused by spindle aberrations, but the origin of breaks and translocations remains elusive. To determine whether one mechanism can bring about both types of instability, we studied the relationship between DNA damage and spindle defects. Although lacking apparent repair defects, primary *Dido* mutant cells formed micronuclei containing damaged DNA. The presence of centromeres showed that micronuclei were caused by spindle defects, and cell cycle markers showed that DNA damage was generated during mitosis. Although the micronuclei themselves persisted, the DNA damage within was repaired during S and G2 phases. DNA breaks in *Dido* mutant cells regularly colocalized with centromeres, which were occasionally distorted. Comparable defects were found in *APC* mutant cell lines, an independent system for spindle defects. On the basis of these results, we propose a model for break formation in which spindle defects lead to centromere shearing.

centrosome | chromosome instability | double-strand break | H2A.X

Most solid tumors show changes in chromosome number, a phenomenon termed aneuploidy, which is caused by chromosome segregation errors and rarely observed in normal cells (1). Many tumors not only gain or lose whole chromosomes, but also accumulate intragenic mutations, thought to suppress negative control on proliferation. Mathematical models predict that chromosomal instability initiates tumorigenesis before the mutation of tumor suppressor genes, underlining the importance of aneuploidy (2). Other studies indicate that aneuploidy is required for sporadic carcinogenesis and collaborates with intragenic mutations by generating multiple copies of mutated chromosomes (3).

Because of their capacity to initiate and propagate intragenic mutations, DNA breaks are considered important in carcinogenesis (3). To examine the origin of breaks, several studies have analyzed the link between cancer and the repair of double-strand DNA breaks (DSBs) (4). But even though mutation of DSB repair genes results in DNA damage after irradiation, little effect was found in untreated cells (5, 6). In addition, sporadic carcinomas bear few if any mutations in DSB repair genes, and many tumor samples show augmented instead of reduced repair activity (7, 8). The role of DSB repair in de novo generation of structural defects thus remains uncertain.

Another potential route for DSB generation involves the mitotic spindle. Spindle defects, an important cause of aneuploidy (1), are frequent in solid tumors, and background γH2A.X levels correlate well with aneuploidy (9). γH2A.X has also been observed after the induction of mitotic arrest by spindle disruption (10, 11). When combined with chromosome end-to-end fusions, the mitotic spindle can damage chromosomes by a mechanism termed the breakage–fusion–bridge (BFB) cycle (12, 13). Still, it remains unclear whether chromosome breakage in the BFB cycle is caused by the spindle itself or by contraction of the midbody actin ring. Inactivation of genes that control the metaphase checkpoint causes severe spindle defects and generally is lethal due to extensive aneuploidy (14). In this study, we used primary cells bearing a mutated *death inducer obliterator* (*Dido*) gene. The main product of the *Dido* gene, Dido3, is a structural protein that localizes to the spindle pole in mitosis (15) and to the synaptonemal complex in meiosis (16). The *Dido* mutation compromises the spindle metaphase checkpoint, leading to an increased frequency of aberrant anaphases (17). Although they suffer from myelodysplastic/myeloproliferative diseases (18), *Dido* mutant mice are viable and can thus provide a cellular model in which to study downstream effects. For a second model, we used colon cancer cell lines lacking a functional *adenomatous polyposis coli* (*APC*) gene. APC is a microtubule-associated protein that regulates spindle dynamics and microtubule–chromosome attachments (19).

We encountered DSBs in micronuclei in *Dido* mutant mouse primary embryonic fibroblasts (MEFs) without signs of DNA damage in the main nucleus. DSBs were found in centromere-containing micronuclei, probably formed by uncorrected merotelic attachments. This shows an aneugenic origin combined with clastogenic effects. Most DSBs in *Dido* mutant MEFs were found adjacent to centromeres, which were occasionally distorted. *APC* mutant cell lines showed similar defects. Thus, two independent models of spindle defects show comparable centromere-localized DSBs. Although mitosis was thought to contribute to chromosomal instability only by chromosome missegregation, our results show that spindle defects can directly generate DSBs. We propose a model in which spindle defects promote tumor formation through several pathways.

Results

Localized DNA Damage in *Dido* Mutant Cells. Primary MEFs from *Dido* mutants show a high frequency of spindle defects and lagging chromosomes (15, 17). When lagging chromosomes persist until mitotic exit, they form micronuclei in the subsequent interphase (20). Aside from spindle defects, faulty repair can generate micronuclei through the loss of centromere sequences (21). To compare micronucleus formation under different conditions, primary MEFs from *Dido*, *Ku80*, and *ATM* mutants were labeled with an antibody to the DSB marker γH2A.X (22), and the frequency of micronuclei was determined (Fig. 1). Ku80 has a critical role in nonhomologous end joining (NHEJ) and ATM is a kinase that phosphorylates several proteins involved in NHEJ and homologous recombination repair (HRR) (23, 24).

A small proportion of wild-type (WT) MEFs contained micronuclei, and this proportion increased in *Dido*, *Ku80*, and *ATM* mutants (Fig. 1*A*). γH2A.X labeling revealed small constitutive γH2A.X foci (6, 25), not related to DSB, in all cell lines. The number

Author contributions: K.H.M.v.W. designed research; A.A.G., M.C.G., N.P.D.-C., J.C.C., and K.H.M. v.W. performed research; V.T., A.F., C.P.-B., and J.C.C. contributed new reagents/analytic tools; C.M.-A. and K.H.M.v.W. analyzed data; K.H.M.v.W. wrote the paper.

The authors declare no conflict of interest.

[1]Present address: Laboratory of Molecular and Cellular Ageing, Institute of Biological Research and Biotechnology, 48 Vas. Constantinou Ave., Athens 11635, Greece.

[2]To whom correspondence should be addressed. E-mail: kvanwely@cnb.csic.es.

doi:10.1073/pnas.0912143106

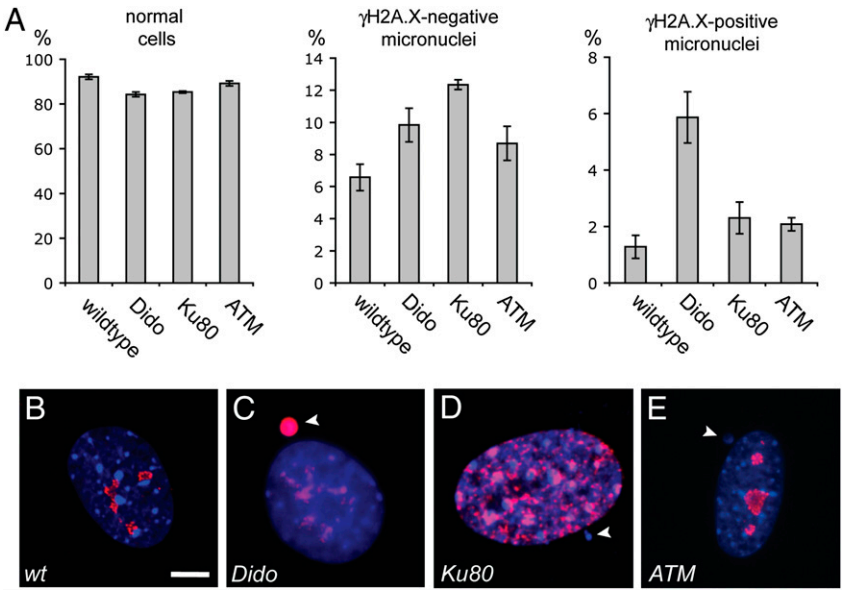

Fig. 1. Localized DNA damage in mutant cells. MEFs were seeded on coverslips, labeled with anti-γH2A.X antibody (red), and studied by fluorescence microscopy. DNA was DAPI stained (blue). Quantitation (*A*) showed an increased proportion of γH2A.X-positive micronuclei in *Dido* mutant MEFs. Error bars indicate standard deviation. (*B–E*) Representative images of WT (*B*) cells and *Dido* (*C*), *Ku80* (*D*), and *ATM* (*E*) mutants are shown. Micronuclei are indicated with arrowheads. Strong γH2A.X labeling was found in micronuclei (*C*), although *Dido* mutant MEFs show no further DNA damage. The weaker signals correspond to constitutive foci not related to DSBs. (Scale bar, 5 μm.)

and localization of constitutive γH2A.X foci is specific for each cell line. Although *Ku80* mutant MEFs show an exceptionally high number of constitutive foci and undue H2A.X phosphorylation in heterochromatic regions, these phenomena are not associated with widespread DSBs. However, untreated WT, *Ku80* mutant, or *ATM* mutant MEFs showed hardly any of the high-intensity γH2A.X label characteristic for DSBs (Fig. 1 *B*, *D*, and *E*). The *Dido* mutation caused a marked (fourfold) increase in micronuclei, many of which with high-intensity γH2A.X labeling (Fig. 1*C*). *Ku80* or *ATM* inactivation, too, increased the frequency of micronuclei, but few of these were γH2A.X positive (Fig. 1 *D* and *E*). γH2A.X-positive micronuclei were also found in *Dido* mutant embryos (Fig. S1), showing in vivo DSB formation. In addition, a subset of *Dido* mutant MEFs showed DNA damage in the main nucleus (Fig S1). In contrast to radiation-induced damage, which gave rise to more or fewer globular regions of γH2A.X (Fig. 2), nuclear γH2A.X regions in *Dido* mutant MEFs were jagged. In conclusion, the *Dido* mutation gives rise to localized DSBs, but repair mutants do not show this kind of "spontaneous" DNA damage.

Normal DSB Repair and H2A.X Phosphorylation in *Dido* Mutant Cells. Even though repair gene mutations cause retention of γH2A.X after DSB induction, no effect is found in untreated cells (5, 6). Untreated *Dido* mutant MEFs, however, formed micronuclei containing damaged DNA. We therefore analyzed the DSB repair efficiency of the *Dido* mutant. Because the *Dido* mutation had no significant effect on overall radiation sensitivity (Fig. S2), DSB kinetics were assayed. MEFs were treated with 2 Gray γ-radiation and labeled with anti-γH2A.X antibodies at different time points (Fig. S3). High-intensity γH2A.X foci were counted to quantify DSBs (Fig. 2*A*). Both WT and *Dido* mutant MEFs showed the rapid appearance of γH2A.X foci after irradiation and gradually lost these as DSB repair took place. After 8 h, few γH2A.X foci remained in WT and *Dido* mutant MEFs. The number of γH2A.X foci did not differ significantly between WT and *Dido* mutant MEFs at any of the time points. Thus, although *Dido* mutants generated more γH2A.X-positive micronuclei than repair-deficient controls, their DSB repair capacity was comparable to that of WT animals.

Repair proteins are recruited to the actual break sites and thus colocalize with γH2A.X foci after induction of DSBs. To test whether Dido proteins are recruited to DSBs, MEFs were irradiated and labeled with antibodies to Dido and γH2A.X (Fig. 2*B*). Dido distributed heterogeneously in the nucleus but did not colocalize with γH2A.X foci, indicating that *Dido* has no overt role in DSB repair.

Although γH2A.X is used as a marker of DSB formation (22), γH2A.X can be formed without DSBs, such as a normal cell cycle (6, 25) or XY body formation in meiosis (26). To determine whether the γH2A.X in micronuclei is associated with DNA damage, we detected phosphorylation of the HRR protein ATM (27) and terminal transferase dUTP nick end labeling (TUNEL) (28) as supplementary markers. Whenever γH2A.X-positive micronuclei were found in untreated *Dido* mutant MEFs, these always yielded corresponding phospho-ATM and TUNEL signals (Fig. 2 *C* and *D*), confirming γH2A.X as a valid DSB marker. In addition, individual micronuclei were found positive for TUNEL, γH2A.X, and distorted centromeres (Fig. 2*D*). Micronuclei, centromere distortion, and DNA damage may thus share a common origin. Taken together, these data indicate that only de novo DSB generation, but not diminished repair or aberrant H2A.X phosphorylation, can explain the γH2A.X-positive micronuclei.

Micronuclei in *Dido* Mutants Are Caused by Spindle Defects. Micronuclei can have two origins: loss of centromeres due to DNA damage, generating chromosomes no longer recognized by the mitotic spindle and defective kinetochore capture due to anomalies of the spindle itself. Because previous studies showed spindle defects in *Dido* mutants (15), we labeled *Dido* mutant MEFs with antibodies to centromeres and α-tubulin and studied these by confocal fluorescence microscopy (Fig. 3). We detected individual centromeres captured by microtubules from opposite poles (Fig. 3 *A* and *B*), which shows that merotelic attachments cause lagging chromosomes in the *Dido* mutant (29).

Uncorrected merotelic attachments lead to the exclusion of lagging chromosomes from the main nucleus during mitotic exit (21). In such an event, a centromere-positive micronucleus is generated. Centromeres in micronuclei thus are reliable indicators of spindle

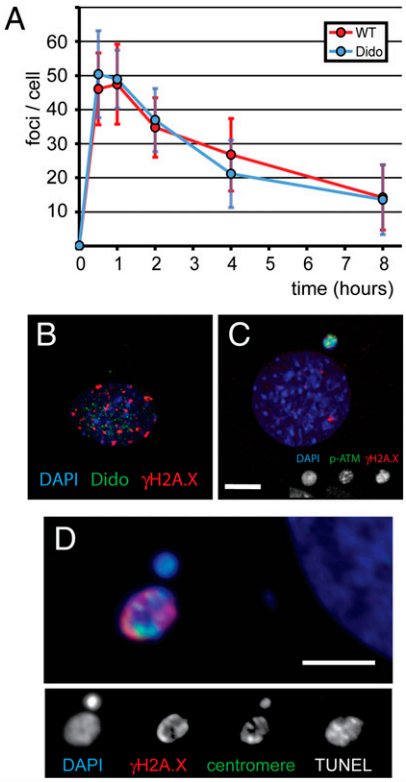

Fig. 2. Normal DSB repair in *Dido* mutant MEFs. (*A*) MEFs from WT and mutant mice were seeded on coverslips, irradiated, and left to recover for the times indicated. Subsequently, cells were fixed, labeled with anti-γH2A.X antibodies, and the number of γH2A.X foci per cell was counted by fluorescence microscopy. Whereas mock-treated controls showed little γH2A.X, a single 2-Gray radiation dose induced ≈50 foci in WT and mutant cells. The number of foci gradually decreased during the 8-h recovery. Wild-type and mutant MEFs showed equal numbers of foci at each time point. Error bars indicate standard deviation. (*B*) Wild-type MEFs were seeded on glass coverslips, irradiated, and labeled with antibodies to γH2A.X and *Dido*. No significant colocalization of the two signals was found. (*C* and *D*) *Dido* mutant MEFs were seeded on glass coverslips and analyzed by phospho-ATM (*C*), or TUNEL and centromere (*D*) labeling, without treatment. DNA was DAPI stained. Colocalization of phospho-ATM or TUNEL with γH2A.X shows that H2A.X phosphorylation characterizes true DSBs. Representative images are shown. (Scale bar, 5 μm.)

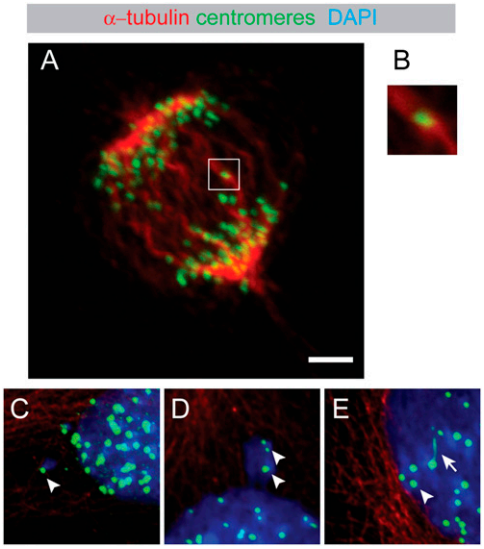

Fig. 3. Merotelic attachments in *Dido* mutant cells. *Dido* mutant MEFs were seeded on coverslips and double labeled with antibodies against centromeres (green) and α-tubulin (red). DNA was stained with DAPI (blue), and cells were studied by confocal fluorescence microscopy. (*A*) Detection of merotelic centromere attachments in *Dido* mutant MEFs. An individual anaphase centromere attached to both spindle poles is shown. The image of a whole cell is from maximum projection (*A*), and the threefold amplification (*B*) is from a single confocal layer. (*C–E*) Appearance of centromeres in *Dido* mutant MEFs. Centromeres in micronuclei (*C*) and in a nuclear protrusion (*D*) are indicated (arrowheads). (*E*) In some cases, an individual centromere is distorted (arrow), whereas neighboring centromeres appear normal (arrowhead). Representative images are shown. (Scale bar, 5 μm.)

defects, but more easily discernible than wrongly attached kinetochores (21, 30). To confirm the origin of micronuclei in the *Dido* mutant, we labeled MEFs with antibodies to centromeres and α-tubulin, and studied these by fluorescence microscopy. Micronuclei in mutant cells were physically separated from the main nucleus, and nearly all (~85%, $n = 120$) contained well-defined centromeres (Fig. 3*C*). Thus, even though the γH2A.X in the micronuclei suggests a clastogenic outcome (breakage), the presence of centromeres demonstrates an aneugenic origin (spindle defects). Uncorrected merotelic attachments can generate enough force to distort kinetochores (29). Accordingly, a small proportion (~15%) of micronuclei in the *Dido* mutant showed a diffuse distorted centromere signal (Fig. 2*D*). In addition, we found distorted individual centromeres adjacent to centromeres that appeared normal (Fig. 3 *D* and *E*). These data confirm merotelic attachments as the probable cause of micronuclei and centromere distortion.

DNA Damage Is Generated During Mitosis. The merotelic attachments and γH2A.X-positive micronuclei indicate a mitotic origin for DSBs. Because standard methods to synchronize cells by itself induce DNA damage (10, 11), we established the time point of DSB generation in nonsynchronized cells. *Dido* mutant MEFs were labeled with antibodies to cyclin B1 and γH2A.X (Fig. 4*A*). Cyclin B1 accumulates in the cytoplasm from S phase to late G2, enters the nucleus at the beginning of mitosis, and is destroyed at anaphase onset (31). γH2A.X-positive micronuclei were regularly found in cells with low cyclin B1 levels characteristic of G1 and early S phase. However, γH2A.X was never found in cells with high cyclin B1, showing absence of DSBs in G2 phase. These data indicate that DNA damage is generated during mitosis, in agreement with break formation after spindle disruption (10, 11) and the mitotic origin of micronuclei (21). The lack of γH2A.X in G2 cells suggests that damage is eliminated during S phase.

To study S phase in more detail, *Dido* mutant MEFs were pulse labeled with bromodeoxyuridine (BrdU) and chased various times with label-free medium (Fig. 4*B*). The combination of BrdU and γH2A.X labeling, showing spatial distribution of constitutive γH2A.X foci (6, 25), allows the discrimination of S phase stages (32). Middle S phase cells, showing a distributed BrdU pattern directly after labeling, were positive for γH2A.X. Micronuclei with low intensity γH2A.X signals were found in middle to late S phase cells, characterized by a distributed BrdU-labeling pattern after a 4-h chase. Out of over 100 examined G2 phase cells, BrdU labeled but without constitutive γH2A.X foci after a 4-h chase, none showed remaining DSBs. Thus, even though the micronuclei themselves persist, the DNA damage within is repaired in S phase. This means that new γH2A.X-positive micronuclei are formed during mitosis. Accordingly, we again found γH2A.X-positive micronuclei after a 14-h chase, when the BrdU-labeled cells had passed through mitosis and were in G1 or early S phase.

Centromere Localization of DNA Damage. Spindle disruption not only generates micronuclei (21), but also causes kinetochore distortion and DNA damage (10, 11, 29), suggesting a common mechanism. The individual micronuclei in *Dido* mutant MEFs, positive for

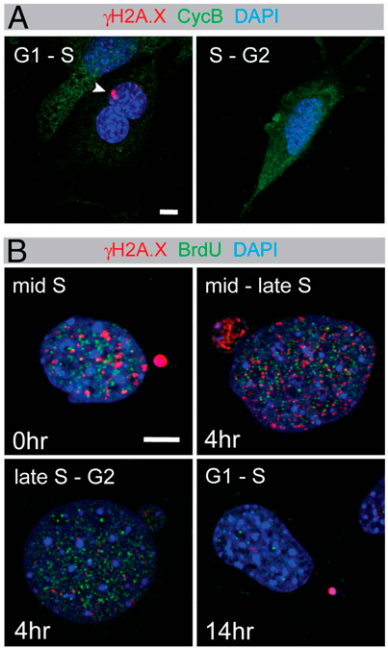

Fig. 4. Intramitotic DNA damage in *Dido* mutant cells. (*A*) MEFs were seeded on coverslips, labeled with anti-γH2A.X and anti-cyclin B1 antibodies, and studied by confocal microscopy. Whereas γH2A.X-positive micronuclei (arrowhead) were found in cyclin B1-negative cells, no γH2A.X was found in cells with a high cyclin B1 content. (*B*) MEFs were pulse labeled with BrdU for 1 h and chased in medium without BrdU for the time indicated. Subsequently, cells were labeled with anti-BrdU (green) and anti-γH2A.X antibodies (red) and studied by confocal microscopy. Micronuclei containing bright γH2A.X labeling were found in early-to-mid S phase cells. Late S phase cells showed micronuclei with diminishing or no γH2A.X. No G2 phase cells were found γH2A.X-positive, but cells that were chased until the next G1 phase again showed γH2A.X in micronuclei. Representative images are shown. (Scale bars, 5 μm.)

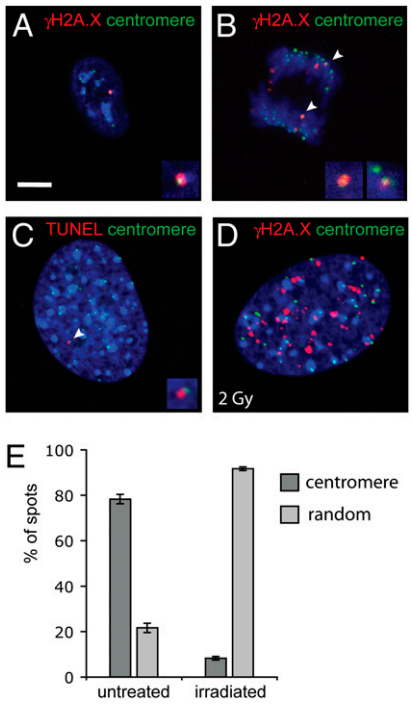

Fig. 5. DSBs in untreated *Dido* mutant MEFs are centromere associated. MEFs were seeded on coverslips, labeled with anti-γH2A.X antibodies (red, *A*, *B*, and *D*) or by TUNEL (*C*), and counter labeled with centromere antibodies (green). Cells were studied by confocal scanning laser microscopy. DNA was DAPI stained (blue). *Insets* show threefold magnification of the centromeric areas (arrowheads). An interphase (*A*) and anaphase (*B*) are shown. (*C*) TUNEL confirmed centromere association of DSBs. Representative images are shown. (*D*) In contrast to spindle-induced breaks, radiation-induced γH2A.X foci do not colocalize with centromeres. (*E*) Quantitation of DSB localization in untreated and irradiated MEFs. Error bars indicate standard deviation. (Scale bar, 5 μm.)

γH2A.X and distorted centromeres, corroborated this hypothesis. To further analyze the hypothesis of spindle-generated DNA damage, we evaluated colocalization of DSBs and spindle attachment sites. *Dido* mutant MEFs were labeled with antibodies to γH2A.X and centromeres and studied by confocal fluorescence microscopy. Whereas one subpopulation of cells showed extensive DSBs in micronuclei (Figs. 1–3), the DNA damage in another subset was restricted to smaller areas (Fig. 5*A*). In nearly all cases, however, γH2A.X surrounded or was adjacent to centromeres. DSBs thus typically localized to the spindle attachment sites on the chromosomes, in agreement with centromere distortion. Mitotic figures showed comparable centromeric γH2A.X labeling (Fig. 5*B* and Fig S4), consistent with a mitotic origin of DNA damage. DSB detection by TUNEL confirmed centromere association (Fig. 5*C*). In contrast to these spontaneous DSBs, few radiation-induced breaks localized to centromeres in *Dido* mutant MEFs (Fig. 5*D*). To quantify the frequency of centromere-associated DSBs under different conditions, we scored the number of γH2A.X foci that colocalized with centromeres. Whereas over 75% of DSBs localized to centromeres in untreated cells, less than 10% of radiation-induced DSBs showed this localization (Fig. 5*E*). Taken together, these results show clear differences between spindle- and radiation-induced γH2A.X and corroborate the role of the mitotic spindle in DSB formation.

To determine whether a deregulated spindle causes DNA damage in an independent model, we confirmed these data in cell lines with a chromosomal instability (CIN) phenotype (Fig. 6 and Fig. S5). These cell lines, bearing a mutated *APC* gene, suffer from aberrant regulation of the cytoskeleton and chromosome segregation defects (19). The CIN cell lines, too, showed γH2A.X adjacent to centromeres, showing that shearing of centromeric chromatin is a common effect of spindle anomalies.

Discussion

Several lines of evidence suggest that aneuploidy is required for sporadic carcinogenesis in mice and collaborates with intragenic mutations during tumorigenesis (2, 3). Aneuploidy is caused by a dysfunctional mitotic spindle (33), but the origins of DNA breaks, which are thought to initiate intragenic mutations, remain poorly understood. Although repair mutants show persistent lesions after DSB-inducing treatments, the same mutations seem to have little or no effect in untreated cells, and mutations in repair genes are

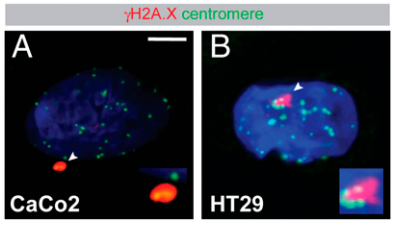

Fig. 6. Centromere-associated DSBs in CIN cell lines. Caco2 (*A*) and HT29 (*B*) cells were seeded on glass coverslips, labeled with antibodies to γH2A.X (red) and centromeres (green), and then analyzed by confocal scanning microscopy. DNA was counterstained with DAPI (blue). Areas indicated with arrowheads are shown magnified twofold in *Insets*. Representative images are shown. (Scale bar, 5 μm.)

rarely found in sporadic tumors (5, 7, 8). In contrast, several lines of evidence implicate the mitotic spindle in DSB generation; genetic or drug-induced spindle abnormalities cause γH2A.X accumulation (10, 11), γH2A.X levels in untreated cells correlate with numerical chromosome instability (9), and cancer cell lines with a CIN phenotype show numerous translocations close to centromeric regions (34).

Here we show that cells with a *Dido* mutation, which causes spindle defects and an increased frequency of lagging chromosomes (15, 17), show localized DSBs in micronuclei, subnuclear regions, and nuclear protrusions. Because these DSBs were found in cells without apparent repair defects, they can only be explained by de novo generation. The micronuclei in *Dido* mutant primary MEFs contained centromeres, indicating an aneugenic (spindle) origin. In addition, we found DSBs adjacent to the centromeres, which form the spindle attachment points in mitosis. In agreement with a role of the spindle, breaks were generated in mitosis and again repaired later in the cell cycle. The *APC* mutants provide an alternative model in which chromosome segregation defects and spindle defects cause aneuploidy (19), confirming DSBs adjacent to centromeres.

The force generated by a single microtubule, ≈50 pN, is not considered enough to overcome the integrity of a DNA helix (35), which breaks at forces around 250 pN in vitro (36). During mitosis, however, microtubules form bundles termed K-fibers to amplify their strength (37). The combination of K-fiber formation and loss of spindle control brings about a potentially dangerous situation, in which the chromosomes are exposed to excessive force. Whereas dicentric chromosomes, the source of the breakage–fusion–bridge cycle, potentially experience the combined force of two K-fibers, lagging chromosomes typically result from a merotelic attachment. Even though merotelic attachments generally do not combine more microtubules than a single K-fiber, uncorrected merotelic attachments are able to overcome the structural integrity of the kinetochore (29). Approximately 15 microtubules connect to a single kinetochore in a merotelic attachment, which can generate a combined force three times the tensile strength of chromosomes (750 pN). Two K-fibers stretch the chromatin between centromeres in the BFB cycle, resulting in anaphase bridges (38). In a merotelic attachment, however, the microtubules act on a single centromere, which lacks the flexibility of intermediate chromatin. Thus, even though merotelic attachments do not generate as much force as two K-fibers, the small dimensions of individual kinetochores favor DNA rupture. Although the merotelic attachments themselves are relatively difficult to detect, distorted centromeres (Fig. 3*F*) point at merotelic attachments as the origin of micronuclei and nuclear protrusions in the *Dido* mutant. Also the isolated centromeric chromosome fragments (Fig. S6), the nuclear protrusions (Fig. S1), and the jagged form of damaged regions (Fig. S1) are consistent with a persistent physical force that shears the chromatin.

In agreement with the appearance of DSBs in arrested cells (11), we found no DNA damage in G2 phase, but detected localized DNA damage as early as prometaphase in mitosis (Fig. S4). These DSBs apparently persisted into the next interphase. Although intramitotic DSBs apparently cause H2A.X phosphorylation (11), they allow for completion of mitosis despite extensive lesions (39). The metaphase–anaphase transition thus seems to be a critical step, as neither spindle symmetry nor chromatin integrity is monitored at this moment (39, 40). This could explain why intramitotic DNA damage does not cause metaphase arrest but allows the cell cycle to continue.

The apparent randomness of structural changes may not reflect random breakpoint positioning, but could result from random transposition of related chromosome fragments (3); small pieces of chromatin consisting almost exclusively of centromeric material could be randomly transposed into noncentromeric sites. Another recurrent genetic defect in carcinomas is the loss or gain of complete chromosome arms (41). Colon cancer cell lines with a CIN phenotype, but not those with other mutations, frequently show this defect (33). The loss of whole chromosome arms is easily explained by centromeric DSBs, as this positions the break exactly at the point that separates the two chromosome arms. After chromosome segregation, free DNA ends with or without centromere identity can react with different partner substrates (Fig. S7). A single event, spindle-induced centromere shearing, may thus underlie a variety of genetic defects found in carcinomas.

Materials and Methods

Cell Culture and Immunofluorescence. *Dido*, *ATM*, and *Ku80* mutant mice have been described (18, 42, 43). All experiments were performed in compliance with the European Union and National Bioethics Committee directives. MEFs were seeded on poly-L-lysine-coated glass coverslips for immunofluorescence. For γH2A.X detection, cells were rinsed briefly in PBS, fixed in PBS containing 4% formaldehyde, and permeabilized in PBS with 0.5% Triton X-100. For tubulin detection, cells were rinsed briefly in PBS and fixed in methanol. After blocking in PBS containing 5% goat serum (1 h, room temperature), cells were incubated with primary antibodies (1 h, room temperature). Cells were then washed, incubated with secondary antibodies (Jackson Immunoresearch), washed again, and mounted in Prolong Gold antifade (Invitrogen). Images were captured on an IX81 laser scanning confocal microscope (Olympus), with sequential fluorophore excitation. Final images were obtained through maximum projection by ImageJ software.

Antibodies. The CREST antiserum, recognizing CENP-A, and antibodies to Dido have been described (16, 44). We used commercial antibodies to γH2A.X (Millipore and Abcam), phospho-ATM (Rockland), cyclin B1 (BD Biosciences), or α-tubulin (Upstate). DNA strand breaks were determined by TUNEL assay, using a fluorescein-dUTP-based in situ cell death detection kit (Roche Diagnostics).

Cell Irradiation. To assay DSB repair, MEFs were seeded on glass coverslips and irradiated with a 2-Gray dose from a calibrated cesium source 24 h after seeding. At the times indicated, coverslips were fixed and pooled for further processing. Cells were labeled with anti-γH2A.X antibodies, counterstained with DAPI, and studied by fluorescence microscopy. The number of γH2A.X foci in 50 cells was counted for each time point.

Bromodeoxyuridine Labeling. To determine cell cycle phase, MEFs were pulse labeled for 1 h with 10 μM BrdU, washed three times in medium without BrdU, and then chased for the times indicated. Cells were fixed, DNA was partially denatured in 50 mM NaOH for 5 min, and BrdU was detected with fluorescein-coupled antibodies (BD Biosciences). DSBs and small constitutive γH2A.X foci were visualized with anti-γH2A.X antibodies, allowing precise S phase determination (32).

ACKNOWLEDGMENTS. The authors thank Dr. Maria Blasco and Dr. Oscar Fernandez-Capetillo for mutant mice, Catherine Mark for editorial assistance, and Almudena Hernando for help during submission. This work was financed by Grants PI05/1965, PS09/0572 (Fondo de Investigación en Salud), and S-BIO-0189-2006 (Comunidad Autónoma de Madrid). K.H.M.v.W. is supported by Grant RyC2004-1886 (Ministerio de Educación y Ciencia). The Department of Immunology and Oncology was founded and is supported by the Consejo Superior de Investigaciones Científicas.

1. Rajagopalan H, Lengauer C (2004) Aneuploidy and cancer. *Nature* 432:338–341.
2. Nowak MA, et al. (2002) The role of chromosomal instability in tumor initiation. *Proc Natl Acad Sci USA* 99:16226–16231.
3. Pihan G, Doxsey SJ (2003) Mutations and aneuploidy: Co-conspirators in cancer? *Cancer Cell* 4:89–94.
4. Agarwal S, Tafel AA, Kanaar R (2006) DNA double-strand break repair and chromosome translocations. *DNA Repair (Amst)* 5:1075–1081.
5. Stiff T, et al. (2004) ATM and DNA-PK function redundantly to phosphorylate H2AX after exposure to ionizing radiation. *Cancer Res* 64:2390–2396.
6. Suzuki K, et al. (2006) Qualitative and quantitative analysis of phosphorylated ATM foci induced by low-dose ionizing radiation. *Radiat Res* 165:499–504.
7. Hosoi Y, et al. (2004) Up-regulation of DNA-dependent protein kinase activity and Sp1 in colorectal cancer. *Int J Oncol* 25:461–468.
8. Pucci S, et al. (2001) Tumor specific modulation of KU70/80 DNA binding activity in breast and bladder human tumor biopsies. *Oncogene* 20:739–747.
9. Yu T, MacPhail SH, Banáth JP, Klokov D, Olive PL (2006) Endogenous expression of phosphorylated histone H2AX in tumors in relation to DNA double-strand breaks and genomic instability. *DNA Repair (Amst)* 5:935–946.

10. Quignon F, et al. (2007) Sustained mitotic block elicits DNA breaks: One-step alteration of ploidy and chromosome integrity in mammalian cells. *Oncogene* 26: 165–172.
11. Dalton WB, Nandan MO, Moore RT, Yang VW (2007) Human cancer cells commonly acquire DNA damage during mitotic arrest. *Cancer Res* 67:11487–11492.
12. Cheung AL, Deng W (2008) Telomere dysfunction, genome instability and cancer. *Front Biosci* 13:2075–2090.
13. Lundblad V (2001) Genome instability: McClintock revisited. *Curr Biol* 11:R957–R960.
14. Dobles M, Liberal V, Scott ML, Benezra R, Sorger PK (2000) Chromosome missegregation and apoptosis in mice lacking the mitotic checkpoint protein Mad2. *Cell* 101:635–645.
15. Trachana V, van Wely KH, Guerrero AA, Fütterer A, Martínez-A C (2007) Dido disruption leads to centrosome amplification and mitotic checkpoint defects compromising chromosome stability. *Proc Natl Acad Sci USA* 104:2691–2696.
16. Prieto I, et al. (2009) Synaptonemal complex assembly and H3K4Me3 demethylation determine DIDO3 localization in meiosis. *Chromosoma* 118:617–632.
17. Rojas AM, et al. (2005) Death inducer obliterator protein 1 in the context of DNA regulation. Sequence analyses of distant homologues point to a novel functional role. *FEBS J* 272:3505–3511.
18. Fütterer A, et al. (2005) Dido gene expression alterations are implicated in the induction of hematological myeloid neoplasms. *J Clin Invest* 115:2351–2362.
19. Kaplan KB, et al. (2001) A role for the adenomatous polyposis coli protein in chromosome segregation. *Nat Cell Biol* 3:429–432.
20. Norppa H, Falck GC (2003) What do human micronuclei contain? *Mutagenesis* 18: 221–233.
21. Mateuca R, Lombaert N, Aka PV, Decordier I, Kirsch-Volders M (2006) Chromosomal changes: Induction, detection methods and applicability in human biomonitoring. *Biochimie* 88:1515–1531.
22. Rogakou EP, Pilch DR, Orr AH, Ivanova VS, Bonner WM (1998) DNA double-stranded breaks induce histone H2AX phosphorylation on serine 139. *J Biol Chem* 273: 5858–5868.
23. Hartlerode AJ, Scully R (2009) Mechanisms of double-strand break repair in somatic mammalian cells. *Biochem J* 423:157–168.
24. Shrivastav M, De Haro LP, Nickoloff JA (2008) Regulation of DNA double-strand break repair pathway choice. *Cell Res* 18:134–147.
25. McManus KJ, Hendzel MJ (2005) ATM-dependent DNA damage-independent mitotic phosphorylation of H2AX in normally growing mammalian cells. *Mol Biol Cell* 16: 5013–5025.
26. Fernandez-Capetillo O, et al. (2003) H2AX is required for chromatin remodeling and inactivation of sex chromosomes in male mouse meiosis. *Dev Cell* 4:497–508.
27. Bakkenist CJ, Kastan MB (2003) DNA damage activates ATM through intermolecular autophosphorylation and dimer dissociation. *Nature* 421:499–506.
28. Gavrieli Y, Sherman Y, Ben-Sasson SA (1992) Identification of programmed cell death in situ via specific labeling of nuclear DNA fragmentation. *J Cell Biol* 119:493–501.
29. Cimini D, et al. (2001) Merotelic kinetochore orientation is a major mechanism of aneuploidy in mitotic mammalian tissue cells. *J Cell Biol* 153:517–527.
30. Kirsch-Volders M, Vanhauwaert A, De Boeck M, Decordier I (2002) Importance of detecting numerical versus structural chromosome aberrations. *Mutat Res* 504:137–148.
31. Pines J, Hunter T (1991) Human cyclins A and B1 are differentially located in the cell and undergo cell cycle-dependent nuclear transport. *J Cell Biol* 115:1–17.
32. Kennedy BK, Barbie DA, Classon M, Dyson N, Harlow E (2000) Nuclear organization of DNA replication in primary mammalian cells. *Genes Dev* 14:2855–2868.
33. Kops GJ, Weaver BA, Cleveland DW (2005) On the road to cancer: Aneuploidy and the mitotic checkpoint. *Nat Rev Cancer* 5:773–785.
34. Abdel-Rahman WM, et al. (2001) Spectral karyotyping suggests additional subsets of colorectal cancers characterized by pattern of chromosome rearrangement. *Proc Natl Acad Sci USA* 98:2538–2543.
35. Alexander SP, Rieder CL (1991) Chromosome motion during attachment to the vertebrate spindle: Initial saltatory-like behavior of chromosomes and quantitative analysis of force production by nascent kinetochore fibers. *J Cell Biol* 113:805–815.
36. MacKerell AD, Jr, Lee GU (1999) Structure, force, and energy of a double-stranded DNA oligonucleotide under tensile loads. *Eur Biophys J* 28:415–426.
37. Maiato H, Sunkel CE (2004) Kinetochore-microtubule interactions during cell division. *Chromosome Res* 12:585–597.
38. Gisselsson D, et al. (2000) Chromosomal breakage-fusion-bridge events cause genetic intratumor heterogeneity. *Proc Natl Acad Sci USA* 97:5357–5362.
39. Skoufias DA, Lacroix FB, Andreassen PR, Wilson L, Margolis RL (2004) Inhibition of DNA decatenation, but not DNA damage, arrests cells at metaphase. *Mol Cell* 15: 977–990.
40. Sluder G, Thompson EA, Miller FJ, Hayes J, Rieder CL (1997) The checkpoint control for anaphase onset does not monitor excess numbers of spindle poles or bipolar spindle symmetry. *J Cell Sci* 110:421–429.
41. Lengauer C, Kinzler KW, Vogelstein B (1998) Genetic instabilities in human cancers. *Nature* 396:643–649.
42. Zhu C, Bogue MA, Lim DS, Hasty P, Roth DB (1996) Ku86-deficient mice exhibit severe combined immunodeficiency and defective processing of V(D)J recombination intermediates. *Cell* 86:379–389.
43. Barlow C, et al. (1996) Atm-deficient mice: A paradigm of ataxia telangiectasia. *Cell* 86:159–171.
44. Kremer L, del Mazo J, Avila J (1988) Identification of centromere proteins in different mammalian cells. *Eur J Cell Biol* 46:196–199.

Supporting Information

SI Text

Intramotitic DNA Damage in Mouse Embryos. *Dido* mutant MEFs bear nuclear regions and micronuclei rich in phosphorylated H2A.X, caused by intramitotic shearing of chromosomes. To confirm that this phenomenon takes place in *Dido* mutant mice and is not an effect of cell culture, embryonary cells were collected by cytospin on day 10.5 post coitum, and labeled with anti-γH2A.X (Fig. S1). We found cells with γH2A.X-positive micronuclei (*A*) or nuclear areas (*B*) in samples from mutant embryos, confirming DNA damage in our model. No micronuclei were found in comparable samples from wild-type mice (data not shown). In addition to the DNA damage in micronuclei, we found γH2A.X in jagged nuclear regions (*C–E*) and nuclear protrusions (*F*) in primary *Dido* mutant MEFs.

DSB Repair in *Dido* Mutant Mice Is Comparable to that of WT Animals. Although the mutation of genes involved in DSB repair pathways frequently results in a markedly increased sensitivity for ionizing radiation (1–3), many of the same mutations cause only mild effects if cells are left untreated. Likewise, mutation of *Ku80* or *ATM* only moderately increased the frequency of γH2A.X-positive micronuclei in our experiments. To test whether the absence of a functional *Dido* gene caused radiation sensitivity, WT and mutant mice were irradiated with a single dose of 7 Gray and monitored for the following 6 weeks (Fig. S2). Because the *Dido* mutation had no significant effect on overall radiation sensitivity, DSB kinetics were assayed. MEFs were treated with 2-Gray γ-radiation and labeled with anti-γH2A.X antibodies at different time points (Fig. S3). Both WT and *Dido* mutant MEFs showed a comparable rapid appearance of γH2A.X foci after irradiation and gradual repair during the recuperation time.

Intramitotic DNA Damage. Whereas some *Dido* mutant MEFs showed extensive γH2A.X in micronuclei, DNA damage was restricted to smaller areas in other cells. Especially cells in mitosis showed this more restricted γH2A.X pattern (Fig. S4). γH2A.X was found as early as prometaphase, indicating that damage can occur as soon as the spindle captures kinetochores. Lesions in telophase cells showed a larger area of H2A.X phosphorylation and noticeable loss of centromere shape.

Evidence of Spindle-Induced DSB in Alternative Models. To determine whether we could detect spindle-associated DNA breaks in other models, we analyzed cell lines with a characterized chromosomal instability (CIN) phenotype. These CIN cell lines, CaCo2 and HT29, bear a mutation in the *APC* gene, which causes spindle defects and aneuploidy (4). In addition, we studied cell lines with no characterized *APC* mutation but with a demonstrated CIN phenotype, HCA7 colon cancer (5) and U2OS osteosarcoma (6) cells.

To detect DNA breaks, cells were seeded on glass coverslips, stained with antibodies to γH2A.X and centromeres, and studied by confocal scanning microscopy (Fig. S5). Just as in *Dido* mutant MEFs, we found breaks adjacent to centromeres in all cell lines tested, although we also detected a few γH2A.X foci with a random localization. Given the fact that these CIN cell lines have been passed for multiple generations in tissue culture, random spots may have a secondary origin such as breakage–fusion–breakage. Taken together, these results show that spindle defects in general are able to cause intramitotic DNA breaks and that these are not restricted to the *Dido* model but can be found in multiple CIN cell lines. Although the U2OS cell line does not bear a mutated *APC* gene, it produces the EWS–FLI fusion, which was recently shown to interact with microtubules (7). The EWS–FLI fusion itself thus may explain the CIN phenotype and centromere-associated DSBs in the U2OS cell line.

Chromosomal Aberrations in *Dido* Mutant Cells. When considered as a single malignancy, carcinomas show a remarkable variety of chromosomal anomalies (8). Carcinoma formation is thought to be a gradual process in which genetic defects accumulate over time. Centrosome amplification and aneuploidy (9), two phenomena found regularly in *Dido* mutant MEFs (10), are characteristic of preinvasive tumors, and thus the early stages of tumorigenesis. At later stages, aneuploidy collaborates with intragenic mutations that suppress negative regulation of the cell cycle (11). We showed here that an effect of centrosome amplification in *Dido* mutant MEFs, a poorly controlled mitotic spindle, can disrupt centromeric chromatin and thereby generate localized DNA damage.

To determine whether centromere-associated chromosome breaks can lead to the apparently random genetic defects observed in full-blown carcinomas, we immortalized *Dido* mutant primary MEFs with human papillomavirus E6 and E7 (12) and studied these cells by spectral karyotyping. Numerical changes were the most apparent alteration in chromosome spreads of immortalized mutant MEFs (Fig. S6); both losses and gains of whole chromosomes were typically observed in a single metaphase. We also found structural aberrations such as translocations, internal inversions bordering the centromere, and loss of chromosome arms. One of the anomalies found was a small chromosome fragment in some metaphase spreads, which may cause the appearance of micronuclei. As we repeatedly found segments derived from the same chromosome and micronuclei consisting almost exclusively of centromeric material, we consider that the small chromosome fragments retain their centromeres.

A Model for the Propagation of Defects During and After Mitosis. Considering that the mitotic spindle caused centromere-associated breaks, additional factors must contribute to the propagation of defects over chromosome arms. We therefore generated a model to include the genetic defects observed in *Dido* mutant MEFs, on the basis of repair during or shortly after chromosome segregation (Fig. S7). Three individual defects were observed by spectral karyotyping:

(*i*) Insertions and translocations. When a small centromeric fragment or chromosome arm is severed from the remainder of the chromosome, this fragment can transpose to a random position, giving rise to a translocation or insertion. When only a small part of centromeric chromatin is carried over in the translocation, the incorporated fragment probably loses its centromeric identity and thus does not create a dicentric chromosome.

(*ii*) Chromosome fragments. An isolated chromosome arm that retains a sufficiently large fragment of centromere will be recognized as a complete chromosome. If repaired by an intrachromosomal end-to-end fusion, a ring chromosome may form. An acentric chromosome arm may replicate, but is easily lost due to its faulty segregation. We found a fragment derived from chromosome 7 in a number of metaphase spreads, indicating that it contains at least a partially active centromere that allows for correct segregation in mitosis.

(*iii*) Internal duplications. When a break within a centromere removes two arms of a chromosome pair during mitosis, the two remaining arms continue to be attached at the centromere and probably form the preferred substrate for repair. Repair of such a break within or adjacent to the centromeric chromatin generates an internal inverted duplication, also termed

isochromosome. Replication then gives rise to a possibly metadicentric chromosome with four identical arms. The fusion of two different chromosomes at the centromere, termed Robertsonian translocation, might have a similar origin.

SI Methods

Spectral Karyotyping. *Dido* mutant MEFs were immortalized with a retroviral vector expressing papillomavirus E6 and E7 and analyzed by spectral karyotyping. Briefly, exponentially growing cells were exposed to 0.1 μg/mL colcemid (2 h, 37 °C) and then harvested. Metaphase chromosomes were dropped on pretreated slides and hybridized according to the manufacturer's protocol (Applied Spectral Imaging). Images (20 metaphases) were acquired with an SD300 Spectra Cube (Applied Spectral Imaging) mounted on a Zeiss Axioplan microscope using a custom-designed optical filter (SKY-1; Chroma Technology).

1. Lavin MF (1999) ATM: The product of the gene mutated in ataxia-telangiectasia. *Int J Biochem Cell Biol* 31:735–740.
2. Essers J, et al. (1997) Disruption of mouse RAD54 reduces ionizing radiation resistance and homologous recombination. *Cell* 89:195–204.
3. Taccioli GE, et al. (1998) Targeted disruption of the catalytic subunit of the DNA-PK gene in mice confers severe combined immunodeficiency and radiosensitivity. *Immunity* 9:355–366.
4. Kaplan KB, et al. (2001) A role for the adenomatous polyposis coli protein in chromosome segregation. *Nat Cell Biol* 3:429–432.
5. Abdel-Rahman WM, Lohi H, Knuutila S, Peltomäki P (2005) Restoring mismatch repair does not stop the formation of reciprocal translocations in the colon cancer cell line HCA7 but further destabilizes chromosome number. *Oncogene* 24:706–713.
6. Al-Romaih K, et al. (2003) Chromosomal instability in osteosarcoma and its association with centrosome abnormalities. *Cancer Genet Cytogenet* 144:91–99.
7. Leemann-Zakaryan RP, et al. (2009) Dynamic subcellular localization of the Ewing sarcoma proto-oncoprotein and its association with and stabilization of microtubules. *J Mol Biol* 386:1–13.
8. Lengauer C, Kinzler KW, Vogelstein B (1998) Genetic instabilities in human cancers. *Nature* 396:643–649.
9. Pihan GA, Wallace J, Zhou Y, Doxsey SJ (2003) Centrosome abnormalities and chromosome instability occur together in pre-invasive carcinomas. *Cancer Res* 63:1398–1404.
10. Trachana V, van Wely KH, Guerrero AA, Fütterer A, Martínez-A C (2007) Dido disruption leads to centrosome amplification and mitotic checkpoint defects compromising chromosome stability. *Proc Natl Acad Sci USA* 104:2691–2696.
11. Pihan G, Doxsey SJ (2003) Mutations and aneuploidy: Co-conspirators in cancer? *Cancer Cell* 4:89–94.
12. Yamashita Y, Tsurumi T, Mori N, Kiyono T (2006) Immortalization of Epstein-Barr virus-negative human B lymphocytes with minimal chromosomal instability. *Pathol Int* 56:659–667.

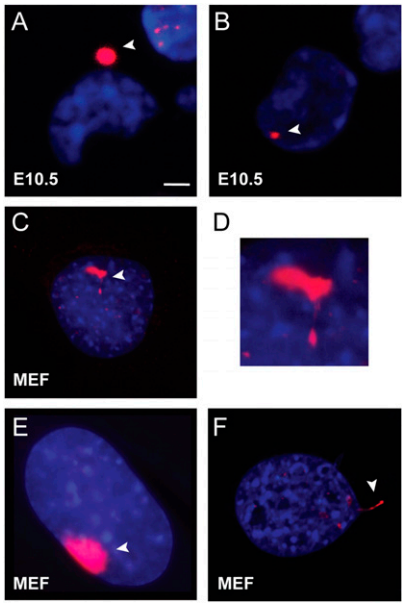

Fig. S1. Localized DNA breaks in *Dido* mutant embryos. Cells were collected on glass coverslips, labeled with antibodies to γH2A.X (red), and analyzed by confocal scanning microscopy. DNA was counterstained with DAPI (blue). A micronucleus (*A*) and nuclear quadrant (*B*) with damaged DNA are shown. γH2A.X was also found in discreet, irregular nuclear regions (*C*–*E*) and nuclear protrusions (*F*) in *Dido* mutant MEFs. (Scale bar, 5 μm.)

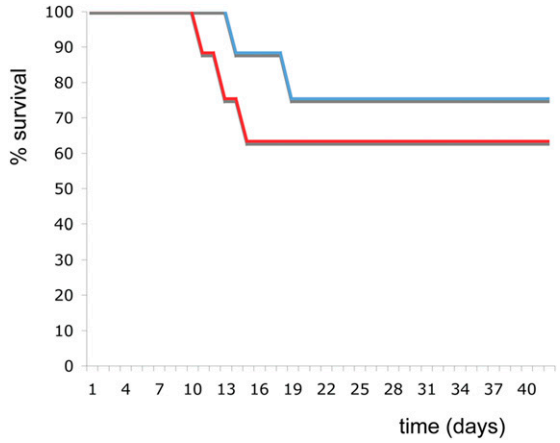

Fig. S2. Absence of radiation sensitivity in *Dido* mutant mice. In each group, eight 3-month-old mice were subjected simultaneously to 7 Gray, and then monitored. Over a period of 6 weeks, comparable numbers of WT (blue line) and *Dido* mutant (red line) mice died. Among the animals that survived the first 3 weeks, no deaths were registered during the monitoring period. The inactivation of genes involved in DSB repair typically causes severe radiosensitivity, which results in the death of all mutant animals after irradiation with doses between 1 and 4 Gray (1–3). Most *Dido* mutant mice, however, survive even a 7-Gray dose, which caused the death of some animals in the control group. These results show that the *Dido* mutation does not result in radiation sensitivity.

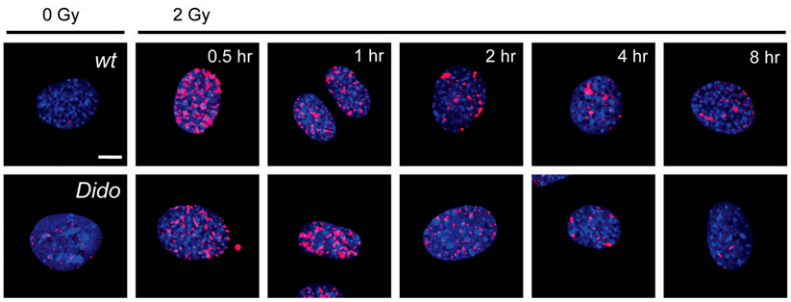

Fig. S3. Normal DSB repair in *Dido* mutant MEFs. (*A*) MEFs from WT and mutant mice were seeded on coverslips, irradiated, and left to recover for the times indicated. Subsequently, cells were fixed, labeled with anti-γH2A.X antibodies (red), and studied by fluorescence microscopy. DNA was DAPI stained (blue). Whereas mock-treated controls showed little DNA damage, a single 2-Gray radiation dose induced ≈50 γH2A.X foci in WT and mutant cells. WT and mutant MEFs showed a comparable gradual decrease in the number of foci during the 8-h recovery. (Scale bar, 5 μm.)

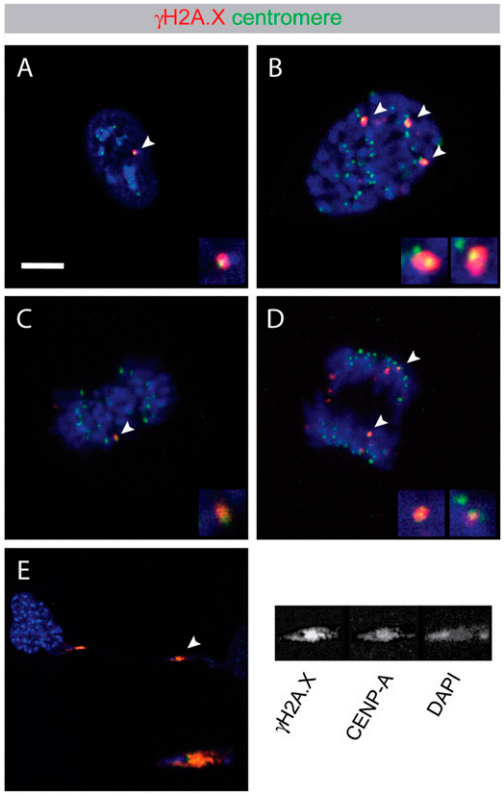

Fig. S4. DSBs in untreated *Dido* mutant MEFs during mitosis. Cells were seeded on coverslips, labeled with anti-γH2A.X (red) and anti-centromere antibodies (green), and then studied by confocal scanning laser microscopy. DNA was DAPI stained (blue). *Insets* show threefold magnification of the centromeric areas (arrowheads). Cell cycle phases are (*A*) interphase, (*B*) prometaphase, (*C*) metaphase, (*D*) anaphase, and (*E*) telophase. The color separation shows colocalization of γH2A.X (*Left*), centromere (*Center*), and DAPI label (*Right*), illustrating a rupture at a centromeric region. (Scale bar, 5 μm.)

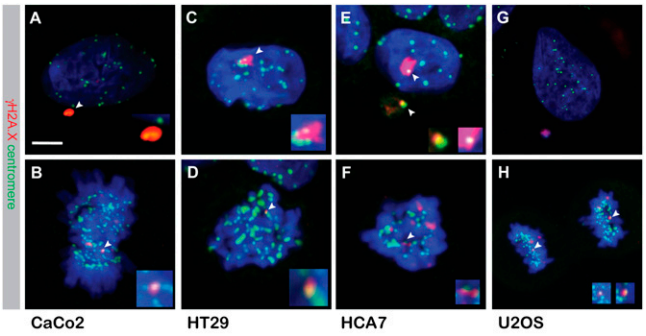

Fig. S5. Localized DNA breaks in CIN cell lines. Cells were seeded on glass coverslips, labeled with antibodies to γH2A.X (red) and centromeres (green), and then analyzed by confocal scanning microscopy. DNA was counterstained with DAPI (blue). Cell lines shown are: Caco2 (*A* and *B*), HT29 (*C* and *D*), HCA7 (*E* and *F*), and U2OS (*G* and *H*). For each cell line, an interphase cell (*Upper*) and mitosis (*Lower*) are shown. Areas indicated with arrowheads are shown magnified twofold in *Insets*. (Scale bar, 5 μm.)

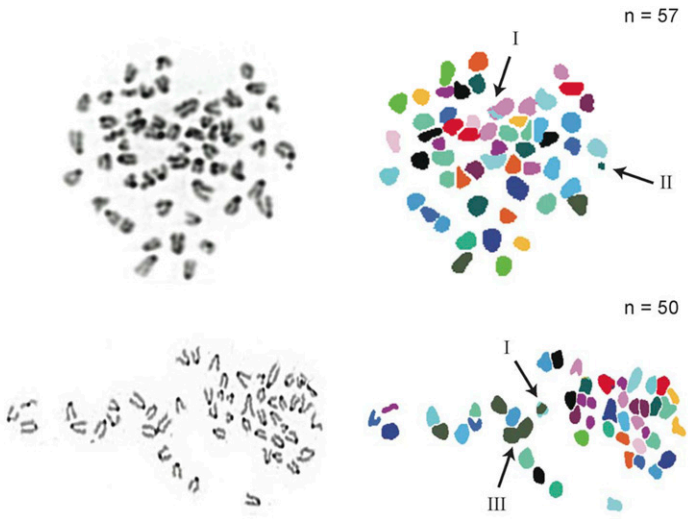

Fig. S6. Genetic defects in *Dido* mutant cells. Metaphase spreads from immortalized *Dido* mutant MEFs were hybridized with chromosome-specific probes and analyzed by spectral karyotyping. Two metaphase spreads are shown (*Left*), with their corresponding hybridization and chromosome number (*Right*). Arrows indicate two translocations (*i*), a small chromosome fragment (*ii*), and an inverted internal duplication (*iii*).

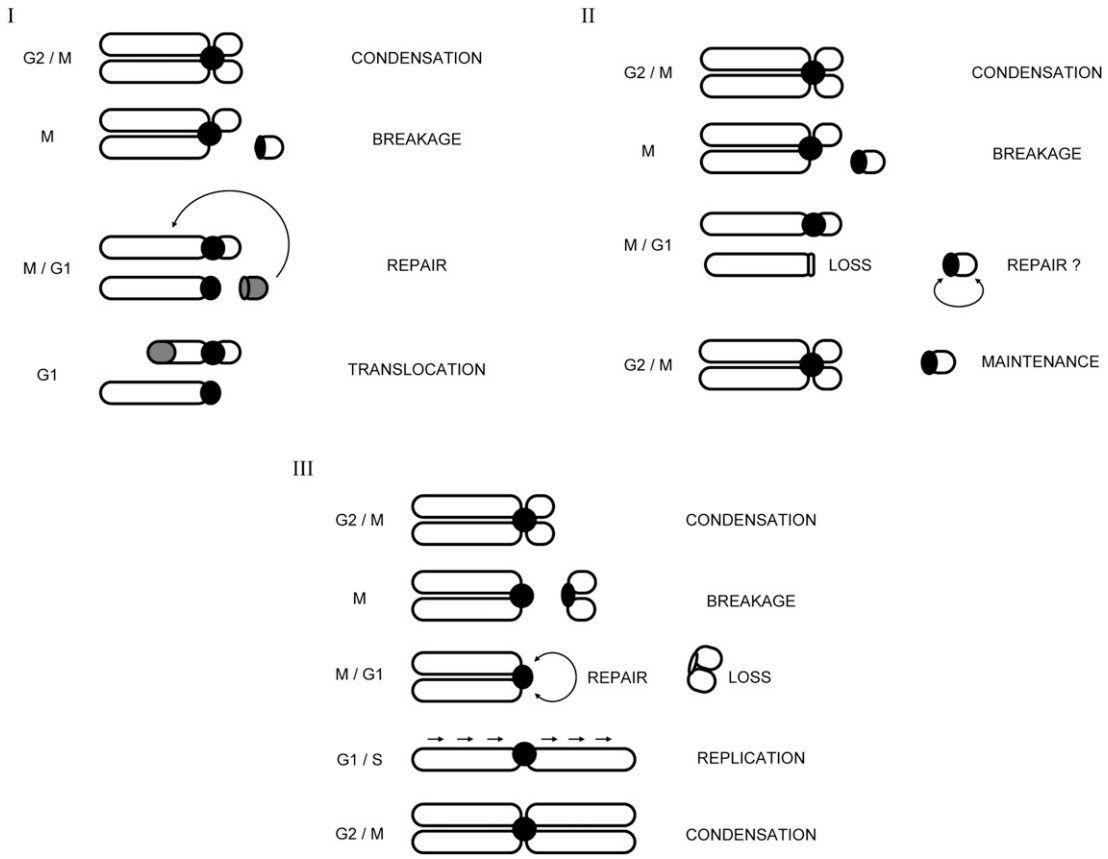

Fig. S7. The structural defects found in metaphase spreads of *Dido* mutant cells can be explained by a single mechanism and differ only in the substrate used for active repair. The main difference between the three examples is the central or lateral location of breaks on the centromere, which determines whether a fragment will maintain its identity as an individual chromosome or will be lost due to defective segregation.